

Photoluminescence characterization of AlGaAs/GaAs test superlattices used for optimization of quantum cascade laser technology

ANNA WÓJCIK-JEDLIŃSKA^{1*}, MICHAŁ WASIAK², KAMIL KOSIEL¹, MACIEJ BUGAJSKI¹

¹Institute of Electron Technology, al. Lotników 32/46, 02-668 Warsaw, Poland

²Institute of Physics, Technical University of Łódź, Wólczajska 219, 93-005 Łódź, Poland

*Corresponding author: awojcik@ite.waw.pl

In this paper, we present the application of photoluminescence spectroscopy as a diagnostic method for evaluation of correctness and homogeneity of AlGaAs/GaAs test superlattices used in the development of quantum cascade laser technology. The structures investigated are used for the growth rate calibration of quantum-cascade-laser structures. The influence of various structural parameters on the observed photoluminescence signal is studied experimentally and theoretically. On the basis of this discussion we analyse spatial uniformity of the epitaxial material over the wafer and diagnose accuracy of the deposition process.

Keywords: photoluminescence spectroscopy, quantum cascade lasers, unipolar devices, semiconductor lasers.

1. Introduction

Quantum cascade lasers (QCLs) [1, 2] are unipolar devices [3], in which an emission of radiation is achieved through the use of intersubband transitions in repeated stack of semiconductor superlattices (SL). The QCL structure contains hundreds of layers that are only a few nanometers thick, and the laser action is possible only when the designed construction is strictly realized. The device realization can be limited either by geometrical and doping inaccuracy or by spatial inhomogeneity of the structure parameters on the epitaxial wafer. Thus, the extreme technological precision is required concerning the individual layer thickness and composition as well as the overall periodicity of the structure. This is assured by atomic monolayer accuracy growth techniques, such as molecular beam epitaxy (MBE) or metal-organic chemical vapor deposition (MOCVD). However, preliminary calibration of a deposition process does not always provide desirable precision due to possible fluctuations in the growth rate or position of the substrate holder, especially when laboratory-type

MBE machines are used. Therefore, additional experimental investigation is needed to determinate the properties and behavior of a given laser wafer [4].

In this paper, we report examination of MBE grown AlGaAs/GaAs QCL structures by means of photoluminescence (PL) spectroscopy. We focused our attention on the optical diagnostics of AlGaAs/GaAs test superlattices, which are used in the development of quantum cascade laser technology. The SL energetic structure (an energetic position, separation and width of individual minibands) is governed by the thickness and composition of individual layers. Since both parameters are linked up during epitaxial process, their influence on the optical properties of the structure investigated is complicated and requires deeper analysis.

2. Experiment

PL measurements are fast and non-destructive diagnostic method, which is extensively used to investigate optical properties associated with band structure in semiconductor structures and devices. This technique is helpful for verification of design foundations as well as for examination of a final epitaxial structure. It should be pointed out that PL measurements concern interband carrier recombination, thus they do not deliver direct information about emission properties of unipolar devices, such as QCLs. However, this technique can be applied to evaluate other optical properties of the structure as well as its quality and homogeneity.

All the experiments reported in this paper were performed at 300 K, in a PL measurement system, the optical arrangement of which is shown in Fig. 1. The PL

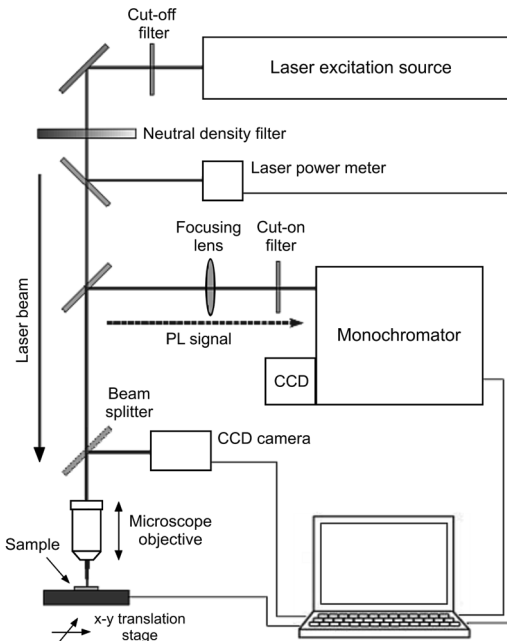


Fig. 1. The optical arrangement of the PL measurement system.

signal from AlGaAs/GaAs structures examined was obtained using excitation of the 514-nm line from an Ar⁺ ion laser. The laser beam was focused on the sample surface by a 10× long-working-distance microscope objective to a spot of about 100 μm in diameter. The laser beam power was monitored using a laser power meter and appropriately reduced by a neutral density filter, so that the excitation did not affect the sample temperature. The sample under investigation was mounted on a vacuum holder to prevent its non-intentional displacement during the measurements. The same microscope objective which focused the excitation beam on the sample surface was also utilized to collect PL signal in back-scattering mode. The collected PL signal was then dispersed using a 0.46-m spectrometer equipped with a grating of 600 lines/mm and detected by a silicon multichannel charge-coupled detector (CCD) cooled to 146 K, which gives a high signal-to-noise ratio.

An additional system equipment is helpful in more advanced PL experiments. The *XY* translation stages equipped with the PC steering encoders ensure remote sample shifting during spatial PL investigation. A digital industrial camera integrated with the microscope allows the sample surface and the excitation laser spot to be monitored during the experiment.

3. Samples

The structures under investigation are different realizations of (GaAs/Al_xGa_{1-x}As) × *n*. The designed Al composition *x* of the constituent layers of the superlattices is 45%, and the lattice periodicity *n* is 100. The structures differ in the well width and barrier thickness. The details of individual samples are listed in the Table. Additionally, the thickness and composition of SL component layers were confirmed by a high resolution X-ray diffractometry (HRXRD). The dynamical diffraction theory has been used for simulating the symmetric (004) reflections, leading to the extraction of structural parameters of periodic structures. About 1% thickness accuracy has been generally achieved for the structures. The barrier layers have been found to contain about 45% of Al, with only a few percent inaccuracy.

All the samples investigated were grown by solid source molecular beam epitaxy (SSMBE) in Riber Compact 21T reactor. The ultrapure beams of the group III elements and the beam of As₄ molecules were generated by using the standard ABN 80 DF effusion cells and by the valved-cracker As effusion cell, respectively. The (100)

Table. The parameters of the Al_xGa_{1-x}As/GaAs SL structures examined: *L_W* – the quantum well width, *L_B* – the barrier thickness, *n* – the number of cells, and *x* – the Al concentration in barriers.

Sample	Superlattice parameters			
	<i>L_W</i> [Å]	<i>L_B</i> [Å]	<i>n</i>	<i>x</i>
#C165	81	46	100	0.45
#C166, #C164	54	46	100	0.45
#C167	81	11	100	0.45

oriented GaAs n^+ substrates supplied by AXT, Inc., were used. The substrate temperature T_s , controlled on the surface of the growing crystal by a pyrometer, was kept at 580 °C. The value of V/III ratio was at least 35 for the growth of both GaAs and $\text{Al}_{0.45}\text{Ga}_{0.55}\text{As}$ layers. The GaAs growth rate V_{GaAs} was adjusted by reflection high energy electron diffraction (RHEED) intensity oscillations before each growth run as equal to 0.5 ML/s. The growth rate V_{AlAs} of AlAs was adjusted to match the 45% of Al content in barriers in the same manner. The corresponding gallium and aluminum fluxes were kept constant during the growth of the whole SL structure. No growth interruptions between the individual layers within the active region were applied, and hence, only the Al effusion cell was regularly activated and closed during the growth run, according to the need.

4. Results and discussion

4.1. The influence of the structural parameters on the optical response

In this section, we analyze the influence of SL constituent layer thickness on the optical features of the structure. As is well-known, variations in structure parameters should be manifested in the PL behavior, through PL peak red- or blue-shifts, signal intensity suppression and/or changes of PL signal shape. This is clearly illustrated by the results of PL measurements performed on three of the SL structures described above. Figure 2 shows the representative room temperature PL spectra. We ascribe the E_{1H} and E_{1L} photoluminescence peak to the radiative recombination of the $n = 1$ heavy hole exciton and to the $n = 1$ light hole exciton, respectively (n denotes the order of the quantized levels involved).

To evaluate the quantum well width effect on a PL spectrum, we compared two signals from the samples of fixed barrier thickness $L_B = 46 \text{ \AA}$ and different wells: $L_W = 81 \text{ \AA}$ and 54 \AA , for samples #C165 and #C166, respectively (Fig. 2a).

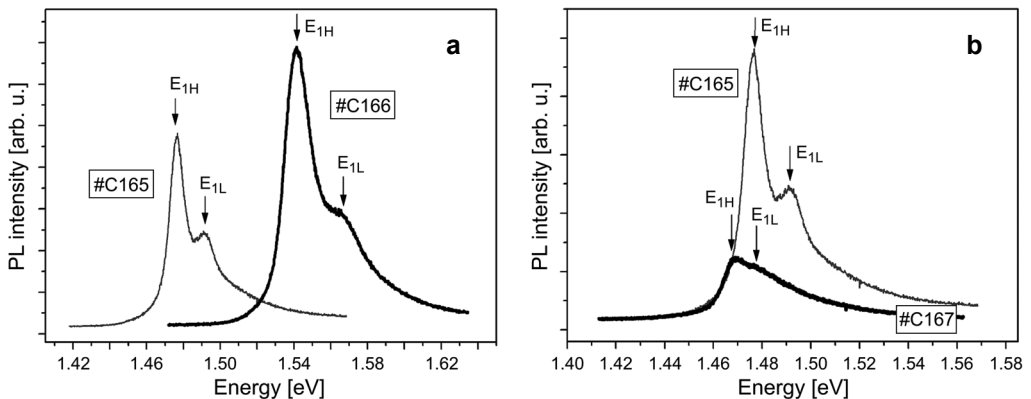


Fig. 2. Photoluminescence spectra of AlGaAs/GaAs SL structures recorded at room temperature: comparison of PL signals from two structures with different quantum well width L_W and the same barriers (a), and different barrier thickness L_B and the same well width (b).

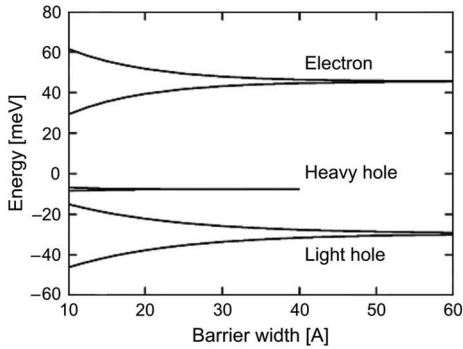


Fig. 3. SL subband dispersion as a function of barrier thickness, calculated for $L_B = 81 \text{ \AA}$ using envelope function approximation.

A pronounced blue-shift of PL signal is observed as L_W decreases. This can be explained as a consequence of the repulsion of the energy levels, like those that happened in a compressively strained single quantum well. The energetic distance between the electron and hole subbands emerging within the SL structure including thin QWs is larger than in the case of the SL of wider QWs. Therefore, the transitions occur with an emission of higher energy radiation and the PL peaks shift to the shorter wavelengths. Additionally, it can be observed that the emission peak becomes stronger when the well thickness decreases.

Figure 2b illustrates the influence of barrier thickness on transition energies in SL structures. We analyzed PL signals from two samples with the same quantum well width ($L_W = 81 \text{ \AA}$) and significantly different barriers ($L_B = 46 \text{ \AA}$ and 11 \AA for samples #C165 and #C167, respectively). As can be noticed, modification of the barrier thickness (keeping barrier composition constant) influences the subband energetic position to a lesser degree than the changes in the well width. Only a slight red-shift is observed in the respective transition energies for the structure of thinner barriers. However, the PL lineshape is significantly changed. The distance between PL peaks corresponding with E_{1H} and E_{1L} transitions decreases as the barriers become thinner. Simultaneously, the overall intensity of PL signal also decreases. Both effects can be explained taking into account the influence of the barrier width on the spatial confinement of the particles in multi-quantum well (MQW) structures. When the barrier is thin the coupling between the carriers of the QWs exists. As L_B decreases, the larger spatial overlap between wave functions gives rise to stronger coupling and results in subband dispersion. This is illustrated in Fig. 3, where we present results of numerical calculations performed for SL structure of a 81 \AA -thick well width.

In general, the width of the subband dispersion depends exponentially on the barrier thickness [5]. For the structure of thinner barriers, the subband dispersion is larger and the difference between $1H$ and $1L$ bands is smaller. This leads to a decrease in the energy separation between E_{1H} and E_{1L} transitions. Thinner barriers result also in poorer localization effect. In consequence, the PL peaks corresponding with E_{1H} and E_{1L} transitions should become wider and the associated energy transitions – less intense. This explains pronounced decrease of the PL signal intensity from sample #C167, in comparison with #C165.

4.2. The homogeneity of the epitaxial structure

Due to transverse distribution of molecular beam intensity, which is an inherent property of MBE technology, the growth rate may be radially non-uniform, which possibly results in inhomogeneity of the deposited layer thickness. It cannot be completely eliminated even in modern types of MBE reactors. Spatially-resolved PL measurements are a simple method used for evaluation of the structure uniformity over the entire epitaxial wafer. Taking into account radial distribution of the structural features of the MBE grown structures the measurements performed along the radius of the wafer provide representative information about the entire sample investigated.

Figure 4 shows the PL spectra of #C164 measured along a radius of a quarter of 2-inch wafer, typically used in test epitaxy processes. It can be observed from the left graph, that the structure demonstrates high homogeneity of its optical response over the entire investigated area. It is more clearly seen on the right graph of Fig. 4, where we compared selected PL spectra, measured in the middle and near the edges of the wafer. The spectral shape of the three spectra presented is very similar. They exhibit a strong PL band peaked at 1.531 eV, which comes from the fundamental recombination between the ground states of the electrons in the conduction subband and the heavy holes valence subband of the GaAs well. The weaker feature seen on the short-wavelength side of the main PL peak, near 1.55 eV, corresponds with the recombination between ground state electrons and light holes. Due to the fact that the optical properties are associated with the band structure we can conclude about

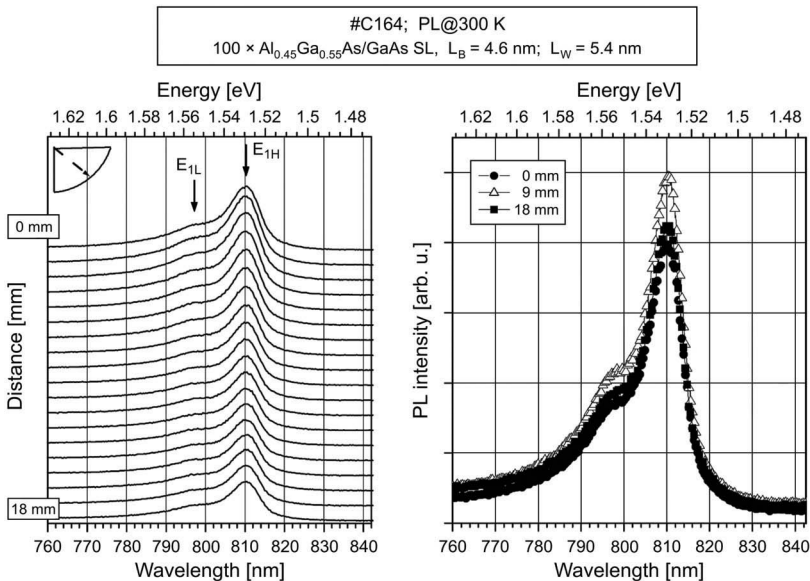


Fig. 4. Distribution of the PL spectra over a quarter of 2-inch epitaxial wafer. High spectral similarity of the measured signals is indicated on the left graph, where three selected PL spectra are compared.

very high structural homogeneity of the sample examined. Lower-intense PL signals measured far from the wafer center indicate slightly poorer crystal quality near the wafer edges and have no effect on the overall valuation of the structure quality.

4.3. Diagnosing the deposition process inaccuracy

Despite a high spatial homogeneity of the structure parameters, which was achieved for MBE grown superlattices, sometimes the differences are observed in optical features of the samples obtained in time distant epitaxial processes. These differences may result from inaccuracy of the deposition preliminary calibration. In Fig. 5, we

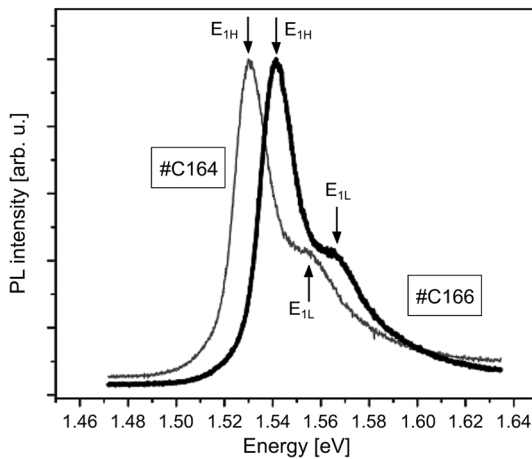


Fig. 5. Comparison of two PL signals from the structures of the same construction, but deposited in two different growth runs.

compared two PL signals from the structures of the same construction, but deposited in two different growth runs. Due to the difference observed between the presented spectra one can conclude about the structural inaccuracy of one of these samples. XRD investigations suggest that it is a result of the thicker QW regions as well as thicker barriers of #C166, compared to #C164. There is about 10 meV difference between respective energy transitions in both samples. However, the presented spectra are very similar regarding the lineshapes. This suggests that the red-shift of the PL spectrum of #C166 is rather due to a wider quantum well layer, which has predominant effect on the energy transitions.

5. Conclusions

We presented the use of photoluminescence spectroscopy as a diagnostic method for evaluating the correctness and homogeneity of AlGaAs/GaAs superlattices for quantum cascade lasers. On the basis of experimental results and theoretical

calculations we discussed the influence of some structural parameters on the optical response of the structures investigated. It has been shown that the quantum well width has strong effect on the energy transitions, whereas changing the barrier thickness results first of all in the PL lineshape modification. We also analysed planar homogeneity of the epitaxial material over the wafer and diagnose inaccuracy of the deposition process. It has been found that the structure grown by SS MBE in Riber Compact 21T reactor for the parameters described in the text has satisfactory optical quality and demonstrates the spatial homogeneity of the structural parameters. Despite that PL measurements do not allow precise determination of the SL constituted layer thickness, this technique is sufficient to evaluate inaccuracy in the structure properties resulting from the epitaxial process, and thus, helpful for proper calibration of the deposition parameters.

Acknowledgements – Michał Wasiak is a scholarship holder of project entitled *Innovative education* supported by European Social Fund. This work has been supported by NCBiR, within the project No. PBZ-MNiSW-02/1/2007.

References

- [1] FAIST J., CAPASSO F., SIVCO D.L., SIRTORI C., HUTCHINSON A.L., CHO A.Y., *Quantum cascade laser*, *Science* **264**(5158), 1994, pp. 553–556.
- [2] SIRTORI C., NAGLE J., *Quantum cascade lasers: the quantum technology for semiconductor lasers in the mid-far-infrared*, *Comptes Rendus Physique* **4**(6), 2003, pp. 639–648.
- [3] KAZARINOV R.F., SURIS R.A., *Possibility of the amplification of the electromagnetic waves in a semicondutor with a superlattice*, *Fizika i Tekhnika Poluprovodnicov* **5**, 1971, pp. 797–800 [*Sov. Phys. Semicond.* **5**, 1971, p. 707].
- [4] KOSIEL K., KUBACKA-TRACZYK J., KARBOWNIK P., SZERLING A., MUSZALSKI J., BUGAJSKI M., ROMANOWSKI P., GACA J., WÓJCIK M., *Molecular-beam epitaxy growth and characterization of mid infrared quantum cascade laser structures*, *Microelectronics Journal* **40**(3), 2009, pp. 565–569.
- [5] BASTARD G., *Wave Mechanics Applied to Semiconductor Heterostructures*, Les Editions de Physique, Les Ulis, France, 1988.

Received June 19, 2009